Dalton
Transactions

RSCPublishing

PAPER

View Article Online
View Journal | View Issue

Cite this: *Dalton Trans.*, 2013, **42**, 484

A new three-dimensional metal–organic framework constructed from 9,10-anthracene dibenzoate and Cd(II) as a highly active heterogeneous catalyst for oxidation of alkylbenzenes†

Dabin Shi,[a,b] Yanwei Ren,[a] Huanfeng Jiang,*[a] Jiaxian Lu[a] and Xiaofei Cheng[a]

Received 13th August 2012,
Accepted 12th September 2012

DOI: 10.1039/c2dt31844j

www.rsc.org/dalton

A novel three-dimensional (3D) porous metal–organic framework, $\{[Cd(\mathbf{L})(H_2O)]\cdot 3H_2O\}_\infty$ (**1**) (**L-H$_2$** = 4,4′-(9,10-anthracenediyl)dibenzoic acid), was synthesized. **1** has a 3D framework formed by **L** connectors and the infinite $\{Cd(O_2CR)_2\}_\infty$ secondary building units (SBUs). Compound **1** was characterized by IR spectroscopy, thermogravimetry, single-crystal, elemental analyses and powder X-ray diffraction methods. We then investigated its adsorption, catalysis and luminescent properties. Framework **1′** exhibits permanent porosity (Langmuir surface area, 324 m^2 g^{-1}), high thermal stability (up to 380 °C), and highly active properties for oxidation of alkylbenzenes. The catalytic results reveal that **1′** is indeed an efficient heterogeneous catalyst with 100% selectivity. To the best of our knowledge, it is the first report that oxidation reactions of alkylbenzenes were performed using Cd(II) with unsaturated coordination spheres as active sites.

1. Introduction

In recent years a new class of microporous materials known as metal–organic frameworks (MOFs) have attracted considerable interest.[1] These compounds are composed of rigid multidentate bridging struts and metal nodes. High micropore volume, large pore sizes, and a high metal content offering potentially valuable active sites are the key features of this new and emerging class of porous materials. Due to the high porosity, the tunable pore size, and functionality, MOFs are potentially useful for applications such as gas storage,[2] chemical sensing,[3] catalysis,[4] and drug delivery.[5] Currently, the study on MOFs as catalysts is one of the hot topics. Although MOF catalysis is a relatively new field, more and more related works were reported by many researchers.[6] The use of MOFs as heterogeneous catalysts is particularly interesting, since the pore size and functionality of the framework can be adjusted over a wide range for a variety of catalytic reactions, namely MOFs can be designed as shape-, size-, chemo-, or enantio-selective catalysts.

So far, a lot of MOFs, which are constructed out of a variety of ligands and cadmium(II), have been extensively documented.[7] In spite of the great potential for these MOFs in heterogeneous catalysis, very few of them have been explored for catalytic applications. For example, Fujita and co-workers for the first time reported cyanosilylation reaction of aldehydes catalyzed by a two-dimensional MOF (layered square grids) of formula $Cd(4,4'\text{-bpy})_2(NO_3)_2$, (bpy = bipyridine).[8] Although Kitagawa and coworkers have also reported Knoevenagel condensation reactions catalyzed by a three-dimensional MOF of formula $[Cd(4\text{-btapa})_2(NO_3)_2]\cdot 6H_2O\cdot 2DMF$ (4-btapa = 1,3,5-benzene tricarboxylic acid tris[*N*-(4-pyridyl)amide]), the active sites of the reaction are not coordinative cadmium(II).[9] In order to obtain catalytically active MOFs, a strategy is that the metal-connecting points with unsaturated coordination environments are used as catalytically active sites.[10] The metal-connecting points in MOFs typically have coordinated water or other small solvent molecules that can be readily removed without destroying the framework structures. Easily, coordinatively unsaturated metal centers can be used to catalyze organic reactions. However, to the best of our knowledge, there have been no reports that the Cd(II) with an unsaturated coordination sphere acts as an active site to catalyze the oxidation of alkylbenzenes in previous literatures related to MOFs containing Cd(II). As is known to all, the development of

---

[a] *School of Chemistry and Chemical Engineering, South China University of Technology, Guangzhou 510640, China. E-mail: jianghf@scut.edu.cn; Fax: +86-20-22236337*

[b] *School of Pharmaceutical Sciences, Zunyi Medical College, Zunyi 563003, China*

† Electronic supplementary information (ESI) available: IR spectra, luminescence spectra, UV-vis spectra, etc. CCDC 890807. For ESI and crystallographic data in CIF or other electronic format see DOI: 10.1039/c2dt31844j

rational approaches to the design of MOFs based on extended carboxylic acids is a subject continually attracting interest in inorganic chemistry. The use of these elongated ligands has given rise to many interesting porous MOFs that possess large-sized channels and high surface area and shows excellent properties.[11] Herein, we used an elongated ditopic carboxylic acid, 4,4′-(9,10-anthracenediyl)dibenzoic acid (**L-H$_2$**), to synthesize a new MOF (**1**), and for the first time utilized **1** based on Cd(II) with unsaturated coordination spheres to catalyze the oxidation reaction of alkylbenzenes.

In this report, a ditopic carboxylic acid (**L-H$_2$**) was used to synthesize a new MOF. A solvothermal reaction between **L-H$_2$** and $Cd(NO_3)_2 \cdot 4H_2O$ in a isopropanol and H_2O mixture afforded yellow crystals with a formula of $\{[Cd(\mathbf{L})(H_2O)] \cdot 3H_2O\}_\infty$ (**1**). The formula was established based on single-crystal X-ray diffraction (XRD) studies, powder X-ray diffraction (PXRD) studies, elemental analysis, and thermogravimetric analysis (TGA) results. Furthermore, we investigated several properties of **1**, such as adsorption, luminescence and catalysis. **1** was activated at 200 °C for 8 h under vacuum, which gave rise to **1′**. The experimental results reveal that **1′** is a highly efficient heterogeneous catalyst with 100% selectivity for the oxidation reaction of alkylbenzenes.

2. Experimental section

2.1. General information

All solvents were purchased from TCI or Alfa and used without further purification. Powder X-ray diffraction (PXRD) patterns were collected on a Bruker D8 powder diffractometer at 40 kV, 40 mA with Cu Kα radiation (λ = 1.5406 Å), with a scan speed of 17.7 s per step and a step size of 0.02° (2θ). Thermogravimetric analyses (TGA) were performed on a Q600 SDT instrument under a flow of N_2 at a heating rate of 10 °C min^{-1} between ambient temperature and 700 °C. Nitrogen and carbon dioxide adsorption experiments were performed with Quantachrome AS-1 MP. Liquid nitrogen was used as coolants to achieve cryogenic temperatures (77 K). The experiments were conducted using ultrahigh-purity N_2 (99.999%) and CO_2 (99.998%). The N_2 sorption isotherms were collected using a pressure range from 10^{-6} atm to 1 atm at 77 K. The CO_2 sorption isotherm was performed at 273 K, using a pressure range of 0.1–1 atm. Elemental analyses for C, H, and N were carried out using a Vario EL III Elemental Analyzer. Room temperature UV/vis spectra measurements were recorded using quartz cuvettes (1 cm) with Teflon stopper on a U-3100 UV/vis spectrophotometer. Luminescence spectra were recorded at room temperature on a Hitachi F-4500 fluorescence spectrophotometer. ^{1}H NMR and ^{13}C NMR were done on a Bruker Model AM-400 (400 MHz) spectrometer. Infrared (IR) spectra were measured from a KBr pellets on a Nicolet Model Nexus 470 FT-IR spectrometer in the range of 4000–400 cm^{-1}. Gas chromatography-mass spectroscopy (GC-MS) spectrometry was recorded on Shimadzu Model GCMSQP5050A system that was equipped with a 0.25 mm × 30 m DB-WAX capillary column.

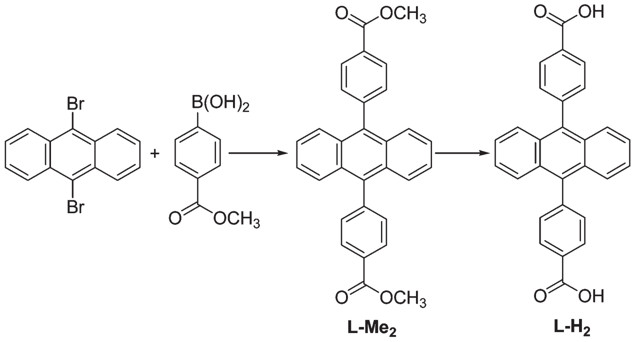

Scheme 1 Synthesis of the ligand **L-H$_2$**.

2.2. Synthesis of ligand[12]

4,4′-(9,10-Anthracenediyl)dibenzoic acid (**L-H$_2$**) was synthesized by a Pd-catalyzed Suzuki coupling between 9,10-dibromo anthracene and 4-(methoxycarbonyl)phenylboronic acid, followed by a base-catalyzed hydrolysis reaction, as shown in Scheme 1.

2.2.1. Synthesis of dimethyl-4,4′-(anthracene-9,10-diyl)-dibenzoate (L-Me$_2$). A mixture of 9,10-dibromo anthracene (5.70 g, 16.96 mmol), 4-methoxycarbonylphenylboronic acid (7.63 g, 42.4 mmol), K_2CO_3 (8.29 g, 60.0 mmol) and palladium tetrakis(triphenylphosphine) (0.51 g, 0.44 mmol, 2.5 mol%), in 140 mL of toluene–CH_3OH–H_2O (8 : 3 : 3) was stirred under nitrogen for 48 h at 100 °C. After the mixture was cooled to room temperature, it was extracted with CH_2Cl_2 and washed with H_2O several times. The organic layer was then dried with $MgSO_4$, and the solvent was removed with a rotary evaporator. The resulting crude product was purified by column chromatography using silica gel and methylene chloride as the eluent. The product was obtained after removal of the solvents (7.08 g, 93.5% yield). ^{1}H NMR ($CDCl_3$): δ = 4.02 (s, 6H), 7.31 (m, 4H), 7.56 (d, 4H), 7.64 (m, 4H), 8.27 (d, 4H). ^{13}C NMR ($CDCl_3$): δ = 52.35 (2C), 125.41 (4C), 126.56 (4C), 129.42 (2C), 129.77 (4C), 131.49 (4C), 136.36 (4C), 139.42 (2C), 144.01 (2C), 167.04 (2C). Anal. Calcd (%) for $C_{30}H_{22}O_4$: C 80.70; H 4.97; found (%): C 79.7; H 5.5.

2.2.2. Synthesis of 4,4′-(9,10-anthracenediyl)dibenzoic acid (L-H$_2$). NaOH (20.0 g) was added to a suspension of 5.0 g of dimethyl-4,4′-(anthracene-9,10-diyl)dibenzoate in 130 mL of dioxane–H_2O (ratio 10 : 3) and the mixture was stirred under reflux for 24 h at 90 °C. The solvent was removed under vacuum, and then H_2O was added to the residue. The mixture (yellow clear solution) was stirred at room temperature for 2 h. The pH value was adjusted to 2 using concentrated HCl. The resulting yellow solid was collected by filtration, washed with water, HCl (1 M), and diethyl ether, and then dried under vacuum. Yield: 4.6 g, 98%. ^{1}H NMR (d_6-DMSO): δ = 7.42 (m, 4H), 7.58 (d, 4H), 7.63 (m, 4H), 8.25 (d, 4H), 13.19 (s, 2H). ^{13}C NMR (d_6-DMSO): δ = 126.4 (4C), 126.0 (4C), 128.4 (4C), 129.2 (4C), 130.6 (2C), 131.2 (4C), 136.2 (2C), 142.6 (2C), 167.5 (2C). Anal. Calcd (%) for $C_{28}H_{18}O_4$: C 80.37; H 4.34; found (%): C 79.4; H 4.62.

2.3 Synthesis of $\{[Cd(L)(H_2O)]\cdot 3H_2O\}_\infty$ (1)

A mixture of **L-H$_2$** (21 mg, 0.05 mmol) and $Cd(NO_3)_2\cdot 4H_2O$ (34 mg, 0.1 mmol) was dissolved in a solvent mixture of isopropanol–H_2O (5.0 mL : 5.0 mL) in a 25 mL Teflon-lined autoclave and heated at 180 °C for 2 days, then cooled at 5 °C every 1 h to room temperature. Yellow crystals of a single phase were obtained. The product was isolated by decanting the mother liquor and washing with the mixture of isopropanol (15 mL) and H_2O (15 mL) (3 × 10 mL). The yield of the reaction, determined from the weight of the solvent-free material (14.5 mg), is 48.0% based on **L-H$_2$**. Anal. Calcd (%) for $C_{28}H_{24}O_8Cd$: C, 55.98; H, 4.03; Found: C, 55.79; H, 4.10. IR data (KBr pellet, ν/cm^{-1}): 3445 (vs), 3064 (w), 1587 (m), 1526 (m), 1390 (vs), 854 (s), 773 (m), 668 (m) (see ESI, Fig. S10†).

2.4. Crystal structure determinations

Single-crystal XRD analyses of complexes **1** was performed on a Rigaku Model Mercury CCD diffractometer operated at 90 kV and 50 mA, using Mo Kα radiation (λ = 0.71073 Å) at room temperature. The empirical absorption corrections were performed using the CrystalClear program.[13] The structures were solved by direct methods and refined on F^2 by full-matrix least-squares technique using the SHELX-97 program package.[14] The single Cd atoms in the asymmetric unit were located first, followed by the other atoms in the main framework (O and C) from the Fourier difference map. All non-hydrogen atoms were refined with anisotropic displacement parameters. Except the solvent molecules, hydrogen atoms attached to carbon were placed in geometrically idealized positions and refined using a riding model. The chemical formulas of **1** was determined using a combination of TGA, elemental analysis, and single-crystal XRD studies. Cambridge Crystallographic Data Centre file CCDC 890807 contains the supplementary crystallographic data for this paper. A summary of the crystal data and relevant refinement parameters for compound **1** are given in Table 1.

Table 1 Crystal data and structure refinement parameters of compound **1**

Compound	**1**
Empirical formula	$C_{28}H_{24}O_8Cd$
Formula weight	609.82
Temperature (K)	293
Wavelength (Å)	0.71073
Crystal system	Monoclinic
Space group	*C*2/*c*
a (Å)	33.321(7)
b (Å)	9.807(2)
c (Å)	7.8951(16)
β (°)	96.68(3)
Volume (Å^3)	2562.4(9)
Z	4
Density (calcd. g cm^{-3})	1.581
Absorption coeff. (mm^{-1})	0.906
F(000)	1220
θ range data collection	3.33–27.46
Limiting indices	$-41 \le h \le 43, -11 \le k \le 12, -10 \le l \le 10$
Reflections collected	12 124
R(int)	0.0413
Data/restraints/parameters	2930/0/174
Goodness-of-fit on F^2	1.126
Final *R* indices [$I > 2\sigma(I)$]	R_1 = 0.0409, wR_2 = 0.0915
R indices (all data)	R_1 = 0.0637, wR_2 = 0.1220

2.5. Catalytic experiments

The oxidation of alkylbenzenes was carried out in a 20 mL test tube at atmospheric pressure and 70 °C, using acetonitrile as a solvent (5 mL). Typically, a mixture of alkylbenzene (0.5 mmol), **1′** (0.013 g, 0.025 mmol), *t*-BuOOH (2.0 mmol), and 5 mL of acetonitrile was heated at 70 °C for 12 h. After cooled to room temperature, the mixture was then filtered and the filtrate was analyzed with gas chromatography-mass spectrometry (GC-MS) (using 1,3,5-trimethylbenzene as an internal standard).

3. Results and discussion

3.1. Crystal structures

Single-crystal X-ray structure determination of **1** reveals a three-dimensional (3D) framework that crystallizes in monoclinic space group *C*2/*c*. Each asymmetric unit contains half of the **L** ligand, half of one Cd atom, and half of one coordinated H_2O molecule. Each carboxylate group of the **L** in tridentate (κ^1–κ^2–μ_2) fashion bridges between two Cd(II) ions, coordinating κ^1- to one and κ^2- to the other (see Fig. 2a). Each Cd(II) is 7-coordinate and bonds to two κ^1-carboxylates, two κ^2-carboxylates and a H_2O molecule (see Fig. 1). Selected bond lengths and angles are given in Table 2. The bridging carboxylate groups link the Cd(II) ions into infinite chains, which contain non-bonded Cd–Cd contacts of 3.98 Å. These chains can be regarded as infinite $\{Cd(O_2CR)_2\}_\infty$ SBUs (see Fig. 2b), which are cross-linked by the **L** ligands into the three-dimensional network (see Fig. 2c). The topological analysis of **1** shows that the 3D net has a vertex symbol ($5\cdot 6^5$) (see Fig. 2d).

Compound **1** has open channels along the *c* crystallographic direction, with one channel opening of 9.80 Å × 38.57 Å (the distance measured between Cd(II) centers) (see Fig. 1c). PLATON calculations[15] of **1** indicate a void volume of 522.7 Å^3 (20.4% of the unit cell volume of 2562.4 Å^3) that is filled with three H_2O molecules. Consistent with this finding,

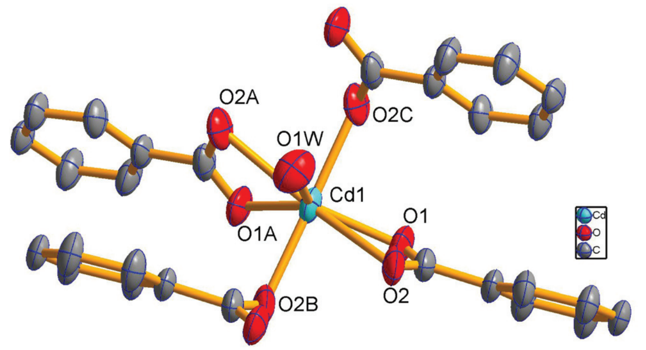

Fig. 1 The coordination environment of Cd1 in **1**. Atoms having "A" and "B" in their labels are symmetry generated. Symmetry code: A: −*x*, *y*, 0.5 − *z*; B: −*x*, 1 − *y*, 1 − *z*; C: *x*, 1 − *y*, 0.5 + *z*.

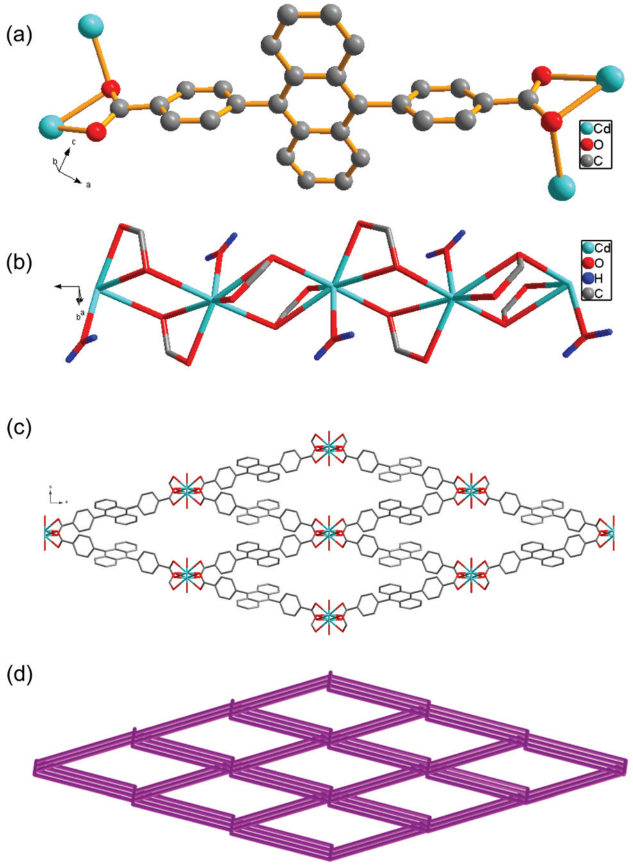

Fig. 2 (a) Representation of coordination modes of **L** ligand. (b) Infinite chains of Cd(II) metal clusters. (c) Stick model of **1** as viewed along the *c* axis. (d) The topological structure of **1**. Cd (light blue), carbon (gray), hydrogen (deep blue) and oxygen (red).

the TGA analysis of **1** showed a solvent weight loss of 12.0% in the 20–110 °C temperature range (calc. 11.9%).

3.2. Thermogravimetric and X-ray power diffraction (XRPD) analyses

Thermal gravimetric analysis (TGA) was carried out under nitrogen atmosphere to examine the stability of the framework. The TGA curve shows a weight loss of 12.0% from 20 °C to 110 °C corresponding to the loss of coordinated water molecules and disordered water molecules in the channels (calc. 11.9%) and then an intense weight loss from ~380 °C, which is attributed to the decomposition of the framework and which ended after 600 °C to give a total weight loss of ~82.0% (see Fig. 3). The pure compound **1** was confirmed by powder X-ray diffraction (PXRD) measurement in which diffraction peaks of experimental data is in excellent agreement with the simulated data from single-crystal X-ray data (see Fig. 4b). We then performed the PXRD measurement of **1′** (see Fig. 4c). The results still match very well with simulated data, indicating no obvious structural change, which demonstrates that **1** possesses permanently stable microporosity.

Table 2 Selected bond lengths [Å] and angles [°] for compound **1**[a]

Bond lengths		Bond angles	
Cd(1)–O(1W)	2.253(5)	O(1W)–Cd(1)–O(1)#1	126.88(9)
Cd(1)–O(1)#1	2.274(3)	O(1W)–Cd(1)–O(1)	126.88(9)
Cd(1)–O(1)	2.274(3)	O(1)#1–Cd(1)–O(1)	106.23(17)
Cd(1)–O(2)#2	2.423(4)	O(1W)–Cd(1)–O(2)#2	89.00(8)
Cd(1)–O(2)#3	2.423(4)	O(1)#1–Cd(1)–O(2)#2	84.94(12)
Cd(1)–O(2)	2.538(3)	O(1)–Cd(1)–O(2)#2	96.26(11)
Cd(1)–O(2)#1	2.538(3)	O(1W)–Cd(1)–O(2)#3	89.00(8)
Cd(1)–C(1)#1	2.747(4)	O(1)#1–Cd(1)–O(2)#3	96.26(11)
Cd(1)–C(1)	2.747(4)	O(1)–Cd(1)–O(2)#3	84.94(12)
O(1)–C(1)	1.262(6)	O(2)#2–Cd(1)–O(2)#3	178.00(16)
O(1W)–H(1W)	0.82	O(1W)–Cd(1)–O(2)	77.93(8)
O(2)–C(1)	1.256(6)	O(1)#1–Cd(1)–O(2)	146.98(12)
O(2)–Cd(1)#2	2.423(4)	O(1)–Cd(1)–O(2)	54.02(11)
C(1)–C(2)	1.497(5)	O(2)#2–Cd(1)–O(2)	72.98(11)
C(2)–C(7)	1.377(6)	O(2)#3–Cd(1)–O(2)	106.59(10)
C(2)–C(3)	1.379(6)	O(1W)–Cd(1)–O(2)#1	77.93(8)
C(3)–C(4)	1.388(5)	O(1)#1–Cd(1)–O(2)#1	54.02(11)
Cd(1)–O(2)#3	2.423(4)	O(1)–Cd(1)–O(2)#1	146.98(12)
C(3)–H(3)	0.93	O(2)#2–Cd(1)–O(2)#1	106.59(10)

[a] Symmetry mode for **1**: #1 $-x$, y, $-z + 1/2$; #2 $-x$, $-y + 1$, $-z + 1$; #3 x, $-y + 1$, $z - 1/2$.

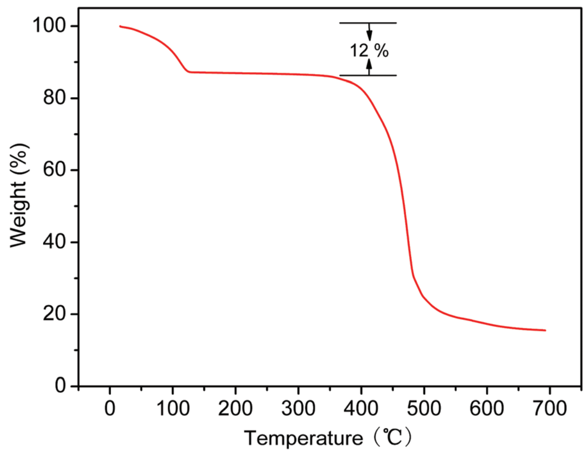

Fig. 3 Thermogravimetric analysis (TGA) curve for **1**. The sample was heated to 700 °C at a heating rate of 10 °C min^{-1}.

3.3. Gas sorption

We have determined the permanent porosity of **1** by nitrogen adsorption at 77 K, as well as the carbon dioxide uptake capacity at 273 K. The N_2 adsorption isotherm of **1** reveals type I behavior (see Fig. 5). From these data, the apparent surface area was calculated using the Langmuir method to be 324 m^2 g^{-1} (225 m^2 g^{-1} BET), thus confirming the permanent porosity of **1**. The CO_2 gas adsorption property of **1** was investigated. The result shows that CO_2 uptake is ~18.5 cm^3 g^{-1} (0.83 mmol g^{-1}) at 273 K at 1.0 atm (see Fig. 6). In contrast, the CO_2 storage capacities of some highly porous MOFs are in the range of 17–55 cm^3 g^{-1} under the same conditions.[16]

3.4. Fluorescent properties

The UV-visible light (UV/vis) spectra properties of **1** and **L-H$_2$** were investigated at room temperature. Compound **1** exhibits a

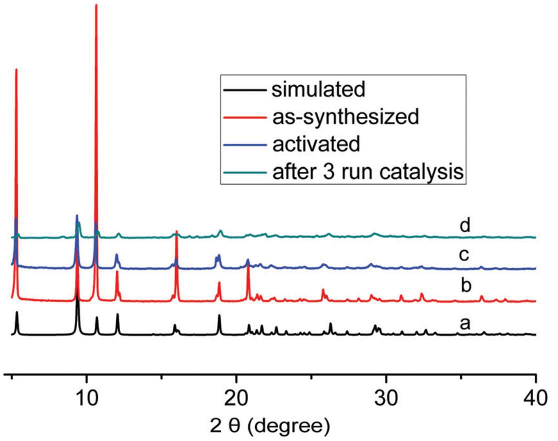

Fig. 4 Powder X-ray diffraction patterns of **1**. (a) **1** simulated patterns from single-crystal structure. (b) **1** as-synthesized pristine sample. (c) **1′** (**1** activated sample at 200 °C for 8 h). (d) **1′** after a 3 run catalysis cycle.

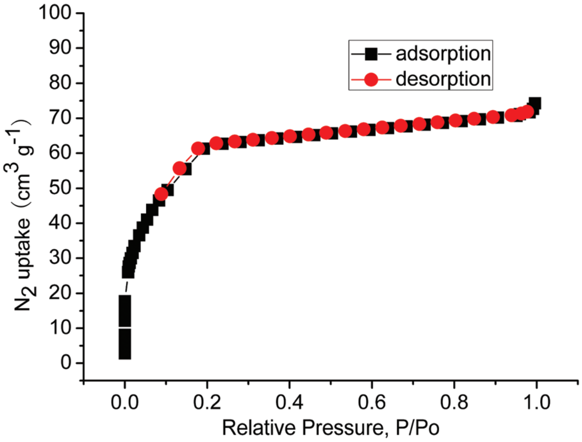

Fig. 5 Nitrogen adsorption isotherm of **1** at 77 K (solid black squares, adsorption; solid red circles, desorption).

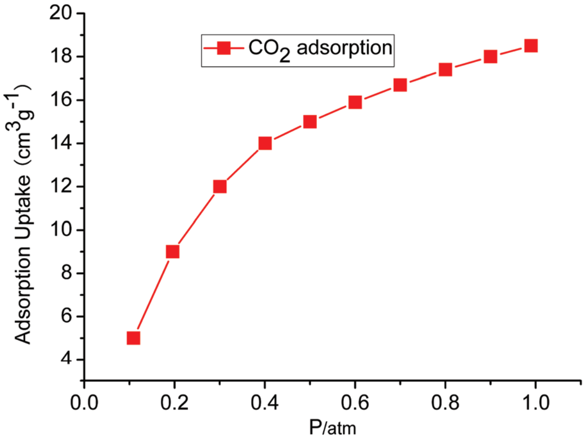

Fig. 6 Carbon dioxide adsorption isotherms at 273 K for the activated **1**.

maximum absorption band at 380 nm in the solid state. The **L-H$_2$** sodium salt aqueous solution (1.0×10^{-5} M) displays strong absorption bands in the UV spectral region from 200 to 400 nm, in which the absorbance maxima are 250 and 365 nm, which are attributed to the n–π* and π–π* transition of the aromatic rings, respectively. Subsequently, the fluorescent properties of **1** and **L-H$_2$** were also investigated at room temperature. As for **1**, the excitation wavelength of 380 nm was set from the absorption band determined from the UV/vis spectral data in the solid state. Compound **1** in the solid state displays an emission maximum at 468 nm. While exciting at 365 nm, the **L-Na$_2$** fluoresces in aqueous solution (1.0×10^{-5} M) with an emission maximum at 425 nm. The results indicate that **1** and **L** possess violet and green fluorescent properties, respectively (see ESI, Fig. S6–S9†).

3.5. Catalytic properties

The oxidation of alkylbenzenes is a very important commercial process for the production of oxygen-containing compounds such as alcohols, aldehydes, ketones, and carboxylic acids.[17] However, the reactions are frequently unselective, and the reaction occurs often under homogeneous conditions, which would lead to several problems, such as difficulty in separation and recovery and disposal of spent catalysts. According to the structural features of **1**, the oxidation reaction of alkylbenzenes, in which **1′** was used as a desirable heterogeneous catalyst, has been investigated. As far as **1** is concerned, as coordinated H_2O molecules are removed, the Cd active sites are completely exposed in the 1D channels along the *c* crystallographic direction (see Fig. 2c). In order to confirm the removal of coordinated H_2O molecules, an as-synthesized pristine sample **1** (0.2038 g) of accurate weight was evacuated at 200 °C for 8 h and **1′** (0.1777 g) was obtained. The result shows a weight loss of **1** (0.0261 g), corresponding to 11.8% of the pristine sample, in accordance with TGA results. **1** was activated at 200 °C for 8 h under vacuum, to remove coordinated H_2O molecules before the reaction. Oxidation reactions of alkylbenzenes using *t*-BuOOH as an oxidant were performed at 70 °C for 12 h. The results of the catalytic oxidation of different substrates were summarized in Table 3. Oxidation of ethylbenzene (EB) was conveniently performed as a control experiment. In all cases, no conversion was observed when the reaction was performed without compound **1′** or using NaClO or H_2O_2 as the oxidant (see Table 3, entries 1–3). When the as-synthesized pristine sample **1** was used as catalysts, GC-MS (using 1,3,5-trimethylbenzene as an internal standard) analysis showed that only one product, acetophenone, was formed with the yield of 7.6% (see Table 3, entry 4). Under standard reaction conditions, the oxidation of ethylbenzene (EB) occurs with a 92.6% yield for acetophenone and the turnover number (TON) is 18.5 (see Table 3, entry 5). These results indicate that the Lewis acidic nature of the coordinatively unsaturated Cd(II) is responsible for the catalytic process. As for **1**, it is very important to obtain the catalytic activity by removing coordinated H_2O molecules. The oxidation of 4-bromoethylbenzene occurs with a 91.4% yield for the corresponding ketone and the turnover number (TON) is 18.3 (see Table 3, entry 6). Under the same catalytic conditions, catalyst **1′** can also

Table 3 Selective oxidation of alkylbenzenes for the formation of ketones[a]

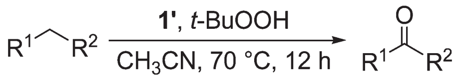

Entry	Substrate	Product	Yield[b] (%)	TON[c]
1[d]	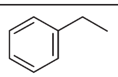	—	Trace	—
2[e]	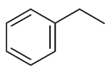	—	Trace	—
3[f]	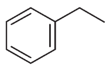	—	Trace	—
4[g]	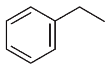	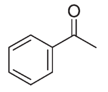	7.6	1.5
5	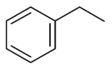	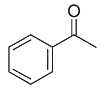	92.6	18.5
6	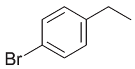	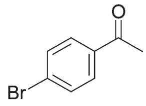	91.4	18.3
7	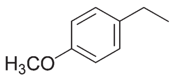	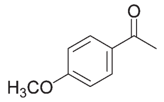	>99%	20
8	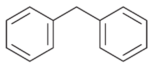	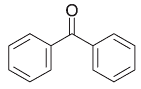	>99%	20
9	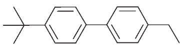	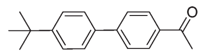	77.2	15.4
10[h]	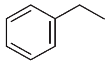	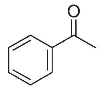	86.5	17.3

[a] Conditions: a mixture of alkylbenzenes (0.5 mmol), **1**′ (0.025 mmol) and *t*-BuOOH (2 mmol) in acetonitrile (5 mL) was stirred at 70 °C for 12 h. [b] Determined by GC-MS (using 1,3,5-trimethylbenzene as an internal standard). [c] TON = (moles of substrate consumed)/(moles of **1**′). [d] Without **1**′. [e] Using NaClO as oxidant. [f] Using H_2O_2 as oxidant. [g] Using the as-synthesized pristine sample **1** as catalyst. [h] The third cycle.

oxidize 4-ethylanisole and diphenylmethane, giving rise to the corresponding ketones in nearly 100% yields with 100% selectivity (see Table 3, entries 7 and 8). In this case, the turnover number (TON) is 20. Maybe electron-donating groups (*e.g.*, methoxyl) contribute to the oxidation conversion. With the size extension of the substrates, a lower yield (77.2%) was obtained in the cases of 4-(4-*t*-butylphenyl) ethylbenzene, which suggests that large substrates are difficult to enter into the channels, relative to small ones (see Table 3, entry 9). Lately, Wu and co-workers have also reported that a porous metalloporphyrinic framework (ZJU-18) exhibits highly efficient and selective oxidation of alkylbenzene. However, the catalytically active sites are based on a Mn^{III}-porphyrin rather than the metal-connecting points with unsaturated coordination environments.[18]

The recyclability of catalyst **1**′ was examined on the oxidation of ethylbenzene. After the oxidation reaction, the catalyst was separated from the reaction mixture by centrifugation, thoroughly washed with acetonitrile, then dried at 200 °C for 8 h under vacuum, and then reused as catalyst for the next run under the same conditions. After a run, the reaction yield is 91.8% for acetophenone. Then after the second run, the reaction yield is 89.2% for acetophenone. Even after the third run, the reaction yield is also up to 86.5% and the turnover number (TON) is 17.3, without an obvious decrease (see Table 3, entry 10). Notably, the catalyst can be recycled and reused several times without any loss of activity. In order to confirm the stability of **1**′, PXRD measurements were conducted on the catalyst after the third run recycle experiment. As shown in Fig. 4d, although the intensity of the diffraction peaks is different, the position of the diffraction peaks of the experimental data is in excellent agreement with the simulated data from single-crystal X-ray data, indicating that the crystalline structure of **1**′ is preserved. To further verify the heterogeneity of the reaction, an experiment was carried out to check for the possible occurrence of any leaching. First, after a standard reaction has taken place for 6 h with the conversion of 67.2% for acetophenone, the mother liquor was split into two fractions, in which one had the solid catalyst while the other was without the solid catalyst. After an additional 6 h, the conversion rates of two fractions are 91.7% (with the solid catalyst) and 69.6% (without), respectively. As for the latter, It was noticed that the percentage conversion was slightly increased to 69.6% after 6 h and this additional 2.4% should be due to catalysis caused by traces of Cd(II) species leached from the solid to the solution. In fact, atomic absorption spectrophotometry (AAS) analysis of the filtrate, after the removal of the catalyst after reaction, confirms that the Cd(II) content is 0.01 mg L^{-1}, corresponding to less than 0.004% of the initial Cd(II) present in the catalyst. The results indicate that **1**′ has good stability during the reaction. From the above studies, we draw a conclusion that **1**′ acts as a heterogeneous Lewis acid catalyst in these oxidation reactions. A plausible mechanism of these oxidation reactions is that unsaturated Cd(II) acts as a Lewis acid active site after coordinated H_2O molecules are removed.

4. Conclusions

In summary, we have successfully synthesized a new 3D MOF using an elongated ditopic carboxylic acid and cadmium salt. Compound **1** is porous and demonstrates CO_2 gas storage and luminescent properties. A catalytically active **1**′ was readily obtained after the removal of coordinated H_2O molecules. Compound **1**′ shows excellent properties for heterogeneous selective oxidation of alkylbenzenes with high yields and 100% selectivity. Notably, the catalyst can be recycled and reused several times without any loss of activity. To the best of our knowledge, it is the first report that oxidation reactions of alkylbenzenes were performed using a MOF that contains Cd(II) with an unsaturated coordination sphere as a catalyst. This work provides an effective pathway for the future synthesis of heterogeneous catalysts with many potential catalysis.

Acknowledgements

We are grateful to the National Natural Science Foundation of China (nos. 20932002 and 21172076), the National Basic Research Program of China (973 Program) (no. 2011CB808600), the Natural Science Foundation of Guangdong Province, China (no. 10351064101000000), and the Fundamental Research Funds for the Central Universities (no. 2010ZP0003) for the financial support.

References

1 (*a*) M. O'Keeffe and O. M. Yaghi, *Chem. Rev.*, 2012, **112**, 675–702; (*b*) W. Morris, B. Volosskiy, S. Demir, F. Gándara, P. L. McGrier, H. Furukawa, D. Cascio, J. F. Stoddart and O. M. Yaghi, *Inorg. Chem.*, 2012, **51**, 6443–6445; (*c*) S. Horike, K. Kishida, Y. Watanabe, Y. Inubushi, D. Umeyama, M. Sugimoto, T. Fukushima, M. Inukai and S. Kitagawa, *J. Am. Chem. Soc.*, 2012, **134**, 9852–9855; (*d*) D. Umeyama, S. Horike, M. Inukai, T. Itakura and S. Kitagawa, *J. Am. Chem. Soc.*, 2012, **134**, 12780–12785; (*e*) P. Horcajada, S. Surblé, C. Serre, D. Y. Hong, Y. K. Seo, J. S. Chang, J. M. Grenèche, I. Margiolaki and G. Férey, *Chem. Commun.*, 2007, 2820–2822; (*f*) P. Horcajada, C. Serre, M. Vallet-Regí, M. Sebban, F. Taulelle and G. Férey, *Angew. Chem., Int. Ed.*, 2006, **45**, 5974–5978; (*g*) H. Wu, Q. Gong, D. H. Olson and J. Li, *Chem. Rev.*, 2012, **112**, 836–868; (*h*) L. Ma, C. Abney and W. Lin, *Chem. Soc. Rev.*, 2009, **38**, 1248–1256; (*i*) Y. Cui, Y. Yue, G. Qian and B. Chen, *Chem. Rev.*, 2012, **112**, 1126–1162; (*j*) J.-P. Zhang, Y.-B. Zhang, J.-B. Lin and X.-M. Chen, *Chem. Rev.*, 2012, **112**, 1001–1033; (*k*) M. Yoon, R. Srirambalaji and K. Kim, *Chem. Rev.*, 2012, **112**, 1196–1231; (*l*) K. Biradha, C.-Y. Su and J. J. Vittal, *Cryst. Growth Des.*, 2011, **11**, 875–886; (*m*) D.-R. Xiao, G.-J. Zhang, J.-L. Liu, L.-L. Fan, R. Yuan and M.-L. Tong, *Dalton Trans.*, 2011, **40**, 5680–5683; (*n*) Z. Yin, Q.-X. Wang and M.-H. Zeng, *J. Am. Chem. Soc.*, 2012, **134**, 4857–4863.

2 (*a*) J.-R. Li and H.-C. Zhou, *Angew. Chem., Int. Ed.*, 2009, **48**, 8465–8468; (*b*) B. Chen, N. W. Ockwig, A. R. Millward, D. S. Contreras and O. M. Yaghi, *Angew. Chem., Int. Ed.*, 2005, **44**, 4745–4749; (*c*) M. Latroche, S. Surblé, C. Serre, C. Mellot-Draznieks, P. L. Llewellyn, J.-H. Lee, J.-S. Chang, S. H. Jhung and G. Férey, *Angew. Chem., Int. Ed.*, 2006, **45**, 8227–8231; (*d*) M. Dincă and J. R. Long, *Angew. Chem., Int. Ed.*, 2008, **47**, 6766–6779.

3 (*a*) B. Chen, L. Wang, Y. Xiao, F. R. Fronczek, M. Xue, Y. Cui and G. Qian, *Angew. Chem., Int. Ed.*, 2009, **48**, 500–503; (*b*) M. D. Allendorf, R. J. T. Houk, L. Andruszkiewicz, A. A. Talin, J. Pikarsky, A. Choudhury, K. A. Gall and P. J. Hesketh, *J. Am. Chem. Soc.*, 2008, **130**, 14404–14405; (*c*) A. Lan, K. Li, H. Wu, D. H. Olsson, T. J. Emge, W. Ki, M. Hong and J. Li, *Angew. Chem., Int. Ed.*, 2009, **48**, 2334–2338; (*d*) S. Pramanik, C. Zheng, X. Zhang, T. J. Emge and J. Li, *J. Am. Chem. Soc.*, 2011, **133**, 4153–4155.

4 (*a*) P. K. Thallapally, C. A. Fernandez, R. K. Motkuri, S. K. Nune, J. Liu and C. H. F. Peden, *Dalton Trans.*, 2010, **39**, 1692–1694; (*b*) C. Zou, Z. Zhang, X. Xu, Q. Gong, J. Li and C.-D. Wu, *J. Am. Chem. Soc.*, 2012, **134**, 87–90; (*c*) S. Horike, M. Dincă, K. Tamaki and J. R. Long, *J. Am. Chem. Soc.*, 2008, **130**, 5854–5855; (*d*) L. Ma, C.-D. Wu, M. M. Wanderley and W. Lin, *Angew. Chem., Int. Ed.*, 2010, **49**, 8244–8248; (*e*) T. B. Liao, Y. Ling, Z. X. Chen, Y. M. Zhou and L. H. Weng, *Chem. Commun.*, 2010, **46**, 1100–1102; (*f*) D. Shi, Y. Ren, H. Jiang, B. Cai and J. Lu, *Inorg. Chem.*, 2012, **51**, 6498–6506.

5 (*a*) P. Horcajada, C. Serre, G. Maurin, N. A. Ramsahye, F. Balas, M. Vallet-Regí, M. Sebban, T. Taulelle and G. Férey, *J. Am. Chem. Soc.*, 2008, **130**, 6774–6780; (*b*) K. M. L. Taylor-Pashow, J. D. Rocca, Z. Xie, S. Tran and W. Lin, *J. Am. Chem. Soc.*, 2009, **131**, 14261–14263.

6 (*a*) D. Saha, R. Sen, T. Maity and S. Koner, *Dalton Trans.*, 2012, **41**, 7399–7408; (*b*) D. Farrusseng, S. Aguado and C. Pinel, *Angew. Chem., Int. Ed.*, 2009, **48**, 7502–7513; (*c*) M. J. Beier, W. Kleist, M. T. Wharmby, R. Kissner, B. Kimmerle, P. A. Wright, J.-D. Grunwaldt and A. Baiker, *Chem.–Eur. J.*, 2012, **18**, 887–898; (*d*) F. X. Llabrés i Xamena, F. G. Cirujano and A. Corma, *Microporous Mesoporous Mater.*, 2012, **157**, 112–117; (*e*) H. Noei, S. Amirjalayer, M. Müller, X. Zhang, R. Schmid, M. Muhler, R. A. Fischer and Y. Wang, *ChemCatChem*, 2012, **4**, 755–759; (*f*) L. T. L. Nguyen, T. T. Nguyen, K. D. Nguyen and N. T. S. Phan, *Appl. Catal., A*, 2012, **425–426**, 44–52.

7 (*a*) S. P. Argent, A. Greenaway, M. del C. Gimenez-Lopez, W. Lewis, H. Nowell, A. N. Khlobystov, A. J. Blake, N. R. Champness and M. Schröder, *J. Am. Chem. Soc.*, 2012, **134**, 55–58; (*b*) H.-L. Jiang, Y. Tatsu, Z.-H. Lu and Q. Xu, *J. Am. Chem. Soc.*, 2010, **132**, 5586–5587; (*c*) Q.-R. Fang, G.-S. Zhu, Z. Jin, Y.-Y. Ji, J.-W. Ye, M. Xue, H. Yang, Y. Wang and S.-L. Qiu, *Angew. Chem., Int. Ed.*, 2007, **46**, 6638–6642; (*d*) X.-R. Hao, X.-L. Wang, Z.-M. Su, K.-Z. Shao, Y.-H. Zhao, Y.-Q. Lan and Y.-M. Fu, *Dalton Trans.*, 2009, 8562–8566; (*e*) M. M. Wanderley, C. Wang, C.-D. Wu and W. Lin, *J. Am. Chem. Soc.*, 2012, **134**, 9050–9053.

8 M. Fujita, Y. J. Kwon, S. Washizu and K. Ogura, *J. Am. Chem. Soc.*, 1994, **116**, 1151–1152.

9 S. Hasegawa, S. Horike, R. Matsuda, S. Furukawa, K. Mochizuki, Y. Kinoshita and S. Kitagawa, *J. Am. Chem. Soc.*, 2007, **129**, 2607–2614.

10 (*a*) A. Dhakshinamoorthy, M. Alvaro and H. Garcia, *Chem. Commun.*, 2010, **46**, 6476–6478; (*b*) A. Dhakshinamoorthy, M. Alvaro and H. Garcia, *Chem.–Eur. J.*, 2010, **16**, 8530–8536.

11 (*a*) H. Furukawa, N. Ko, Y. B. Go, N. Aratani, S. B. Choi, E. Choi, A. Ö. Yazaydin, R. Q. Snurr, M. O'Keeffe, J. Kim and O. M. Yaghi, *Science*, 2010, **329**, 424–428; (*b*) H. Deng, S. Grunder, K. E. Cordova, C. Valente, H. Furukawa, M. Hmadeh, F. Gándara, A. C. Whalley, Z. Liu, S. Asahina, H. Kazumori, M. O'Keeffe, O. Terasaki, J. F. Stoddart and O. M. Yaghi, *Science*, 2012, **336**, 1018–1023.

12 S. Ma, D. Sun, P. M. Forster, D. Yuan, W. Zhuang, Y.-S. Chen, J. B. Parise and H.-C. Zhou, *Inorg. Chem.*, 2009, **48**, 4616–4618.

13 (*a*) *Molecular Structure Corporation, CrystalClear, Version 1.36*, Molecular Structure Corporation (MSC), The Woodlands, TX, USA, 2000; (*b*) *Rigaku Corporation, CrystalClear, Version 1.36*, Rigaku Corporation, Tokyo, Japan, 2000.

14 G. M. Sheldrick, *Acta Crystallogr., Sect. A: Found. Crystallogr.*, 2008, **64**, 112–122.

15 A. L. Spek, *Acta Crystallogr., Sect. A*, 1990, **46**, C34.

16 J. Y. Lee, O. K. Farha, J. Roberts, K. A. Scheidt, S. T. Nguyen and J. T. Hupp, *Chem. Soc. Rev.*, 2009, **38**, 1450–1459.

17 (*a*) F. Yu, P.-Q. Zheng, Y.-X. Long, Y.-P. Ren, X.-J. Kong, L.-S. Long, Y.-Z. Yuan, R.-B. Huang and L.-S. Zheng, *Eur. J. Inorg. Chem.*, 2010, 4526–4531; (*b*) C. Chen, J. Xu, Q. Zhang, Y. Ma, L. Zhou and M. Wang, *Chem. Commun.*, 2011, **47**, 1336–1338; (*c*) M. Balamurugan, R. Mayilmurugan, E. Suresh and M. Palaniandavar, *Dalton Trans.*, 2011, **40**, 9413–9424; (*d*) P. Zhang, Y. Wang, J. Yao, C. Wang, C. Yan, M. Antonietti and H. Li, *Adv. Synth. Catal.*, 2011, **353**, 1447–1451.

18 X.-L. Yang, M.-H. Xie, C. Zou, Y. He, B. Chen, M. O'Keeffe and C.-D. Wu, *J. Am. Chem. Soc.*, 2012, **134**, 10638–10645.